Available online at www.sciencedirect.com
SCIENCE DIRECT®
International Journal of Hydrogen Energy 29 (2004) 1165–1172
International Journal of HYDROGEN ENERGY
www.elsevier.com/locate/ijhydene

Numerical simulation of diffusivity of hydrogen in thin tubular metallic membranes affected by self-stresses

Wu-Shou Zhang[a,*], Min-Qiang Hou[a,b], He-Yi Wang[c], Yi-Bei Fu[c]

[a] *Institute of Chemistry, Center for Molecular Science, Chinese Academy of Sciences, P.O. Box 2709, Beijing 100080, China*
[b] *Graduate School of the Chinese Academy of Sciences, Beijing 100039, China*
[c] *Institute of Nuclear Physics and Chemistry, China Academy of Engineering Physics, Mianyang 621900, China*

Accepted 24 October 2004

Abstract

Based on the self-stress theory for hydrogen in thin tubular shells, we numerically calculate apparent diffusion coefficients (ADCs) of hydrogen in membranes obtained from the time-lag and half-rise methods under chemopotential- and flux-step boundary conditions. It is found that ADCs differ from the diffusion coefficient under stress-free conditions when either the initial concentration or the chemopotential-step (or flux-step) is taken to be a nonzero value. At the same time, effects of other parameters on values of ADC are discussed as well. The theoretical results are qualitatively consistent with the available experimental data. Our results indicate that a small current will give the minimum error in determining the diffusion coefficient while the initial hydrogen content is nonzero.

Keywords: Hydrogen diffusion; Diffusion coefficient; Self-stress; Thin membranes

1. Introduction

Since the discovery of the up-hill diffusion (UHD) effect in hydrogen permeable metals by Lewis et al. [1], there has been much theoretical work concentrated on the aspects of stresses induced by the hydrogen (interstitials) diffusion in metals (solids) [2–8]. However, the appropriate physical pictures of self-stress effects in practical shapes of material have only been given recently [9–12].

In earlier works, we presented models describing self-stresses and related effects produced by hydrogen interstitials in thin shells and circular plates [9–11]. The UHD phenomena, the time courses of pressure change in a tube during hydrogen absorption and interruption of steady diffusion [1,2,13–24] were demonstrated and interpreted by these theories. Besides these phenomena, it has been found that self-stresses lead to changes of apparent diffusion coefficient (ADC) if traditional relations are applied in experiments [1,2,13–26]. This is one of the reasons that ADCs of H in metal (alloy) hydrides differ from one work to another. Because self-stresses are produced by the nonhomogeneous concentration distribution of hydrogen in metals and this is a necessary condition for diffusivity measurement, so self-stresses must affect diffusion processes, hence the diffusivity measurements. Therefore, it is important to diminish or subtract this effect in experiments. On the other hand, effects of self-stress on the transport of hydrogen in metals (alloys) are an important problem in corrosion kinetics, hydrogen storage and other related problems. All these issues form the academic and technological backgrounds of the present subject; we will discuss it using numerical methods based on the model established earlier [9–11].

2. Model

Similar to the previous paper [9], the chemical potential of hydrogen interstitials in a metallic lattice (M) under a stress σ for a dilute solid solution can be expressed as

$$\mu_{\mathrm{H}}(n_{\mathrm{H}}, \sigma) = \mu_{\mathrm{H}}^{0} + RT \ln n_{\mathrm{H}} - V_{\mathrm{H}}\sigma, \quad (1)$$

* Corresponding author. Fax: +86-10-62559373.
E-mail address: wszhang@iccas.ac.cn (W.-S. Zhang).

0360-3199/$ 30.00
doi:10.1016/j.ijhydene.2003.10.007

where μ_H^0 denotes the chemical potential of hydrogen under the reference state; n_H is the atomic ratio of hydrogen to metal; and V_H is the partial molar volume of H in M. Referring to Baranowski et al. [27] and Fukai [28], $V_H = 1.7\ cm^3\ mol^{-1}$ for fcc metals and alloys while $n_H < 0.75$.

Considering hydrogen diffusion across a thin tubular membrane, the induced stress for homogeneous materials is [9]

$$\sigma = \frac{2V_H E C_0}{3(1-\nu)}(\bar{n}_H - n_H) \tag{2}$$

with the average H atomic ratio

$$\bar{n}_H = \frac{1}{L}\int_0^L n_H\,dz, \tag{3}$$

where E is the Young's modulus, $E = 100$–200 GPa; ν is the Poisson's ratio, $\nu = 0.3$–0.4; C_0 is the concentration of H in M corresponding to $n_H = 1$, $C_0 = 0.1$–0.15 mol H cm^{-3} for materials used experimentally [1,2,13–26]; L is the membrane thickness; z is the coordinate along the thickness direction, the upstream side is $z = 0$ (outer surface) and the downstream side is $z = L$ (inner surface). The hydrogen flux has the form

$$J(z,t) = -D_0 C_0(1 + u_\sigma n_H)\frac{\partial n_H}{\partial z} \tag{4}$$

with

$$u_\sigma = \frac{2V_H^2 E C_0}{3(1-\nu)RT}, \tag{5}$$

where D_0 is the stress-free diffusion coefficient (SFDC) of H in M; u_σ is the self-stress factor and is a dimensionless material constant, $u_\sigma = 13$–33 at room temperature utilizing the aforementioned parameters. Applying the mass balance condition to the flux expression, one gives

$$C_0\frac{\partial n_H}{\partial t} = -\frac{\partial J(z,t)}{\partial z}. \tag{6}$$

In this report, we discuss mainly the absorption process. The initial condition is the homogeneous distribution of hydrogen with concentration $n_{H,0}$ in the tube wall and the equilibrium of hydrogen chemical potential approaches between the solid and gas phases in the tube:

$$\mu_H(n_{H,0},0) = \tfrac{1}{2}\mu_{H_2,0}, \quad 0 \leqslant z \leqslant L, \quad t < 0, \tag{7}$$

where $\mu_{H_2,0}$ is the initial value of the chemical potential of H_2 gas.

The boundary conditions depend on the experimental technique applied. For the gas/membrane/gas situation, i.e. only the gas and solid phases are involved [17–22], the boundary condition at the outer surface is [2]:

$$\mu_H(n_H,\sigma) = \mu_H(n_H^*,0) = \tfrac{1}{2}\mu_{H_2}, \quad z = 0, \quad t \geqslant 0, \tag{8}$$

where n_H^* is the H/M ratio under the stress-free condition, μ_{H_2} is the chemical potential of the external H_2 gas. We name this situation as the chemopotential-step [1] and it is equivalent to the first boundary condition (concentration-step) in the stress-free case. It corresponds to pressure step and potentiostatic charging for the gas phase and electrochemical hydrogen absorption, respectively.

In the discussions below, we suppose that the inner volume of the tube is large enough that the chemical potential of hydrogen at the downstream side almost does not change:

$$\mu_H(n_H,\sigma) = \mu_H(n_{H,0},0) = \tfrac{1}{2}\mu_{H_2,0}, \quad z = L, \quad t \geqslant 0. \tag{9}$$

Of course, this isobaric assumption differs from the isometric condition in experiments. However, we must confine our discussion to this ideal situation; otherwise, the diffused flux, boundary condition and other kinetic parameters will depend on the tube volume if it is small.

In the electrolyte/membrane/gas situation, i.e. the outer surface of the tube is in contact with an aqueous solution, there are two extreme boundary conditions depending on the manner of hydrogen charging in experiments. For the potentiostatic charging, the chemopotential-step condition of Eq. (8) is appropriate with $\mu_{H_2}/2$ being replaced by the chemical potential of hydrogen adsorbed on the outer surface. For the galvanostatic charging as used experimentally [1,2,13–16], the corresponding boundary condition is

$$J(0,t) = J_0, \quad z = 0, \quad t \geqslant 0, \tag{10}$$

where J_0 is the applied charging current density. The boundary condition at $z = L$ is the same as Eq. (9) for all these situations.

The amount of hydrogen diffused across the tube wall and collected at the downstream side can be measured by the pressure change in the tube:

$$\Delta p = p - p_0 = \frac{RTA}{2V}\int J_{ex}\,dt, \tag{11}$$

where $J_{ex} = J(L,t)$ is the diffused flux at the exit side, p_0 is the initial hydrogen pressure, A is the area of tube wall involved in the diffusion process, V is the volume into which the diffused hydrogen is collected and the other parameters have their usual meanings.

For the purpose of analytical and numerical treatments, further analysis is carried out in terms of dimensionless variables and equations. Introducing of the following symbols:

$$\xi = z/L, \tag{12}$$

$$\tau = D_0 t/L^2 \tag{13}$$

and

$$j(\xi,\tau) = \frac{LJ(z,t)}{D_0 C_0}. \tag{14}$$

[1] The term 'chemopotential' is utilized to replace 'chemical potential' in this work.

Table 1
Four characteristic times of diffusion across a plate under stress-free conditions [29–32]

Name	Symbol	Definition	Value	
			Concentration-step	Flux-step
Time-lag	τ_L	$\tau - Q/j_{ex}$, $(\tau \to \infty)$	1/6	1/2
Half-rise	$\tau_{1/2}$	$j_{ex}(\tau_{1/2}) = j_\infty/2$	0.138	0.379
Inflection-point	τ_i	$j''_{ex}(\tau_i) = 0$	$0.924/\pi^2$	$1.648/\pi^2$
Break-through	τ_b	$\tau_i - j_{ex}(\tau_i)/j'_{ex}(\tau_i)$	$0.5/\pi^2$	$0.76/\pi^2$

Eqs. (4) and (6) simplify to

$$j(\xi,\tau) = -(1+u_\sigma n_H)\frac{\partial n_H}{\partial \xi} \tag{15}$$

and

$$\frac{\partial n_H}{\partial \tau} = -\frac{\partial j(\xi,\tau)}{\partial \xi}, \tag{16}$$

respectively. Using Eqs. (1) and (2), Eq. (8) is expressed as

$$n_H \exp[u_\sigma(n_H - \bar{n}_H)] = n_H^*, \quad \xi = 0, \quad \tau \geqslant 0. \tag{17}$$

Eq. (10) is transferred to

$$j(0,\tau) = j_0, \quad \xi = 0, \quad \tau \geqslant 0, \tag{18}$$

where $j_0 = LJ_0/D_0C_0$. The quantity of diffused hydrogen across the tube wall is expressed by

$$Q = \int j_{ex}\,d\tau \tag{19}$$

with $j_{ex} = j(1,\tau)$. Thus, Eq. (11) simplifies to

$$\Delta p = \frac{AL}{2V}RTC_0Q. \tag{20}$$

Generally, there are four principal time characteristics to determine the diffusion coefficient under stress-free conditions in experiments as shown in Table 1 [29–32]. The well known is the time-lag τ_L which is defined as the intercept of Q on the τ-axis while the diffusion time is long enough and the permeation flux approaches the steady value j_∞. Another is the half-rise time $\tau_{1/2}$ at which the permeation flux reaches half the value of the steady state. The other two characteristic values, the inflection-point and break-through times, depend on the inflection of current ($d^2j_{ex}/d\tau^2 = 0$) and its tangent with time, their values under stress-free conditions are shown in Table 1 as well.

In self-stress cases, the concepts of τ_L and $\tau_{1/2}$ are valid as shown in Fig. 1, but their values differ from those in Table 1. Hence, a value of ADC obtained from Table 1 generally differs from the SFDC (D_0). In experiments, the applicability of time characteristics is determined by the techniques employed. For gas/membrane/gas and electrolyte/membrane/gas situations, τ_L is easily acquired by the measurement of pressure change; therefore, the time-lag method has been used widely [1,2,13–24]. If an electrolyte

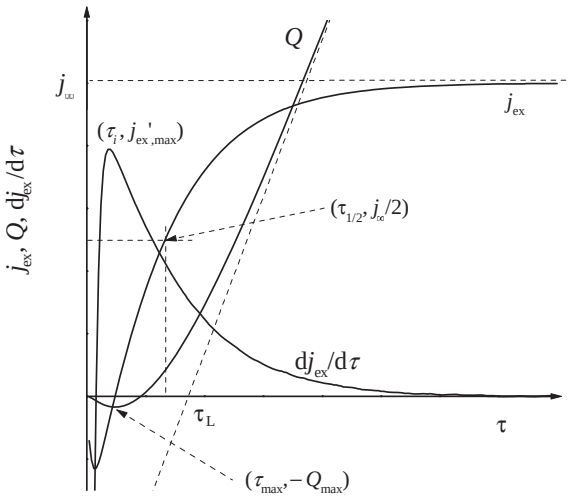

Fig. 1. Schematic picture of UHD effects and characteristic quantities in diffusion of hydrogen across thin tubular membranes.

is introduced in the tube [16], τ_L can be estimated from the potential change and $\tau_{1/2}$ can be evaluated from the anodic current, which reflects the diffused flux. ADCs determined by the time-lag and half-rise methods are defined as

$$\frac{D_L}{D_0} = \begin{cases} \dfrac{1}{6\tau_L} & \text{for chemopotential-step,} \\ \dfrac{1}{2\tau_L} & \text{for flux-step,} \end{cases} \tag{21}$$

$$\frac{D_{1/2}}{D_0} = \begin{cases} \dfrac{0.138}{\tau_{1/2}} & \text{for chemopotential-step,} \\ \dfrac{0.379}{\tau_{1/2}} & \text{for flux-step,} \end{cases} \tag{22}$$

respectively.

On the other hand, although the inflection-point still exists in self-stress experiments, it will induce negative values of ADC using the traditional definition in Table 1 as shown in Fig. 1. Therefore, we do not discuss τ_i and τ_b afterwards.

In this work, we give only the numerical results based on Eqs. (15)–(19) and using the frame reported earlier [33]. In the calculation, the time step is 10^{-6} and the space step is 10^{-2}, and the precision is 10^{-4}. The time-lag under the concentration-step condition is 0.16664 which gives a relative error of 1.6×10^{-4} in comparison with the standard value of 1/6. In the determination of τ_L and $\tau_{1/2}$, $\tau = 3$ is long enough to make the flux approach the steady value.

3. Results

In this section, we discuss the effects of various parameters on ADCs under different boundary conditions. Firstly, we concentrate on the chemopotential-step situation for experiments of gas/membrane/gas [17–22] under pressure-step in gas phase absorption or electrolyte/membrane/gas under potentiostatic charging in electrochemical absorption. Secondly, the flux-step for electrolyte/membrane/gas with galvanostatic charging is discussed [1,2,13–16]. Finally, general situations between these two extreme cases are considered.

3.1. Chemopotential-step

The effects of various parameters on ADCs under chemopotential-step boundary conditions are shown in Fig. 2. Fig. 2(a) demonstrates an example, it is easily found that the self-stresses make j_{ex} and Q decrease in the

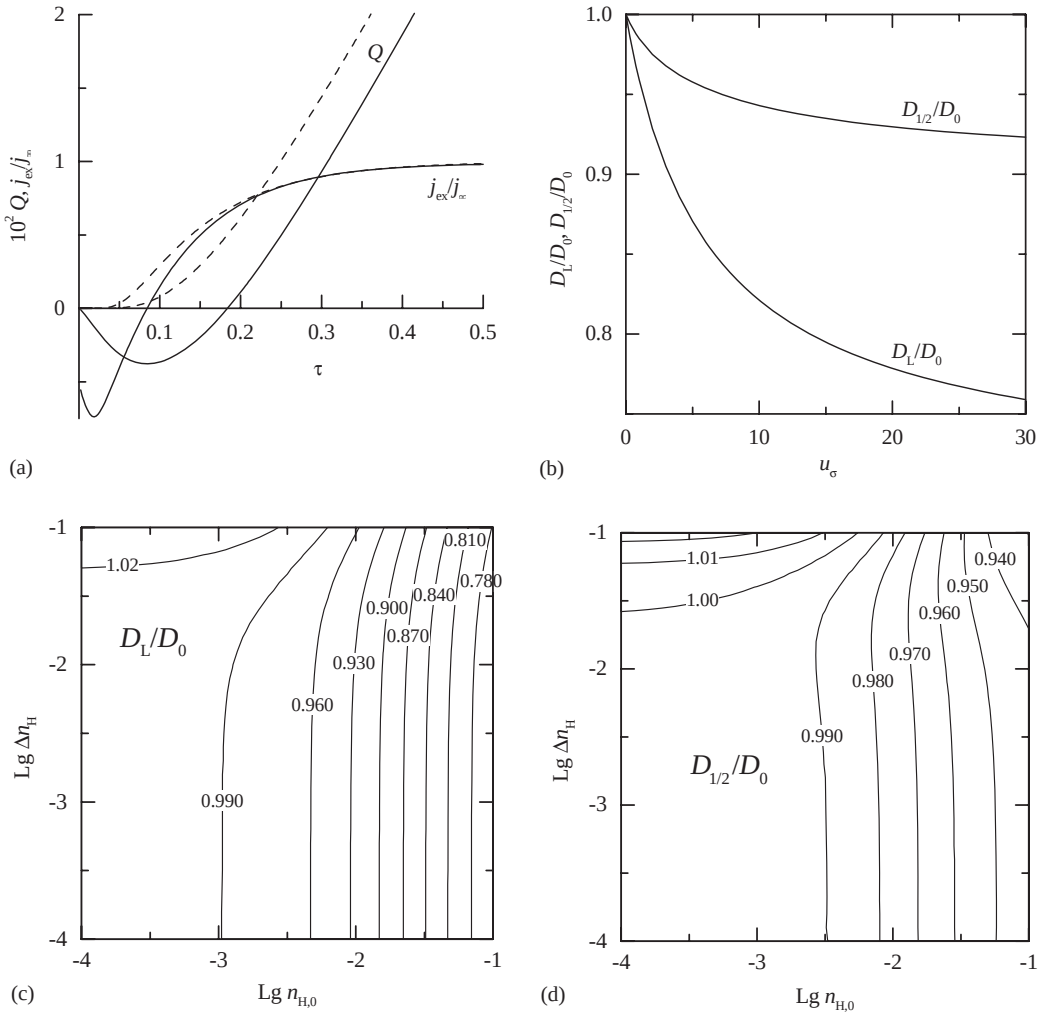

Fig. 2. Effects of various parameters on ADC under chemopotential-step boundary conditions. (a) An example of diffusion flux and diffused quantity for the self-stress (solid curves) and stress-free situations (dashed curves); (b) the effects of self-stress factor u_σ; (c) contour map of D_L vs. $n_{H,0}$ and Δn_H; (d) contour map of $D_{1/2}$ vs. $n_{H,0}$ and Δn_H. The parameters are $n_{H,0} = 0.1$, $\Delta n_H = n_H^* - n_{H,0} = 0.1$, $u_\sigma = 20$ except for independent variables in each figure.

initial period of hydrogen absorption (i.e. UHD) and their increase in tube delays in comparison with the stress-free case, $\tau_L = 0.214$ and $\tau_{1/2} = 0.149$ are all greater than the stress-free values and $D_L = 0.779D_0$ and $D_{1/2} = 0.926D_0$ are all less than D_0.

Fig. 2(b) shows the effects of self-stress factor u_σ; we find that ADCs decrease with increasing u_σ due to the UHD effects. For one sort of metal (or alloy) and a fixed hydrogen concentration, the partial molar volume of hydrogen V_H is constant, so the stress-factor only changes with temperature as indicated by Eq. (5). In other words, ADCs approach the SFDC while the temperature is high enough and ADCs depart from the SFDC while the temperature is low.

Influences of initial hydrogen concentration $n_{H,0}$ and chemopotential-step, which is expressed by the concentration-step under a stress-free condition $\Delta n_H = n_H^* - n_{H,0}$, are shown in Fig. 2(c) and (d). We find that ADCs increase with increasing Δn_H and decrease with increasing $n_{H,0}$ as observed experimentally [20–22]. Contrary to one's expectation, ADCs are greater than the SFDC while $n_{H,0}$ approaches zero and Δn_H is large as observed experimentally [20–22], the reason for this will be given in Section 4. When $n_{H,0} \to 0$ and $\Delta n_H \to 0$, we find that D_L and $D_{1/2}$ approach D_0 as expected.

3.2. Flux-step

The flux-step situation is shown in Fig. 3. Because j_{ex} increases more rapidly under self-stress than the stress-free case after the initial period of hydrogen absorption (see Fig. 3(a)), $\tau_L = 0.434$ and $\tau_{1/2} = 0.333$ are all less than the stress-free values; the corresponding $D_L = 1.152D_0$ and $D_{1/2} = 1.138D_0$ are all greater than D_0. At the same time, ADCs increase with increasing u_σ as shown in Fig. 3(b). This trend is contrary to the chemopotential-step case.

Changing of ADC with $n_{H,0}$ and j_0 is similar to the behaviors of $n_{H,0}$ and Δn_H in chemopotential-step cases as shown in Figs. 3(c) and (d), i.e. ADCs decrease with increasing $n_{H,0}$ and increase with increasing j_0. Another feature is that ADCs are greater than the SFDC as indicated in electrolyte/membrane/gas experiments [13–24]. Similar to Fig. 2(c) and (d), D_L and $D_{1/2} \to D_0$ if only both $n_{H,0} \to 0$ and $j_0 \to 0$; otherwise, ADCs depart from the SFDC.

It must be pointed out, that although the time-lag method under flux-step has been available for some years [29–32], utilizing the value 1/6 but not 1/2 as τ_L has still appeared in galvanostatic charging experiments [2,13,20]. This is one of the reasons why the diffusion coefficients of H in Pd under electrolyte conditions are less than the value in the gas phase experiments by about three times. However, this misleading does not affect the conclusion here.

3.3. General situations

The chemopotential- and flux-step are the extreme situations based on the presumption that the surface processes are so fast that the permeation kinetics is under diffusion control; they can be realized by subtle surface treatments and parameter controlments in experiments. The actual metal (alloy) surface and bulk processes are complex [11,32–35], for example, surface reactions (e.g. the Tafel and Heyrovsky steps) at electrode will diminish the permeation flux during hydrogen absorption [11]. This means that the surface processes must be considered in general situations; these factors in conjunction with the stress effects will induce the measured diffusion coefficient depart prominently from the actual values. Sometimes, numerical simulation has to be used to determine the diffusivity. This is the reason why we do not compare our results with specific experimental data in this work.

In the stress-free situation, we have $1/6 \leqslant \tau_L \leqslant 1/2$ and $0.138 \leqslant \tau_{1/2} \leqslant 0.379$ as shown in Table 1. From Figs. 2 and 3, we also find that the above conclusions are valid except for some special situations (small $n_{H,0}$ and large Δn_H). This means the order of diffusion coefficient value can be estimated even if the self-stress effects are involved for dilute solid solutions ($n_{H,0} < 0.1$ here).

Another similar characteristic for both boundary conditions is that $D_L/D_0 > 1$ and $D_{1/2}/D_0 > 1$ when the applied Δn_H (or j_0) is large but $n_{H,0}$ is very small, which means that measurements of diffusion coefficient must be taken with caution even for dilute solid solutions.

4. Discussion

Changes of ADC are controlled by two opposite and competitive factors. The first one is the term $u_\sigma n_H$ shown in Eq. (4) or (15), which accelerates the diffusion process and makes ADCs greater than the SFDC [33,36]. Although the term n_H is the local value of hydrogen content in solid, only the increment (i.e. Δn_H) has contributed to the flux because the contribution of background (i.e. $n_{H,0}$) has been canceled out by the boundary condition. This conclusion has also been proved by numerical simulation of hydrogen absorbing into a plate under galvanostatic charging [33]; it indicated that self-stress makes half-absorption time is less than the stress-free case although some details of the model differ from here. This could explain the fact ADCs increase with increasing Δn_H and j_0 (see Figs. 2 and 3). Another factor that affects ADCs is the UHD, which makes a metal membrane absorb hydrogen from gas phase at the downstream side and the front of hydrogen flux in the membrane is delayed correspondingly; thus, ADCs may be less than the SFDC. Because self-stresses depend on the nonuniform distribution of hydrogen content, and the chemopotential-step will make hydrogen content at the surface increase faster than the flux-step case, it is easily understood that the chemopotential-step will have a more prominent UHD effect than the flux-step situation. Because the UHD effects increase with increasing $n_{H,0}$, so ADCs decrease with $n_{H,0}$ as shown by Eq. (16) in Ref. [9].

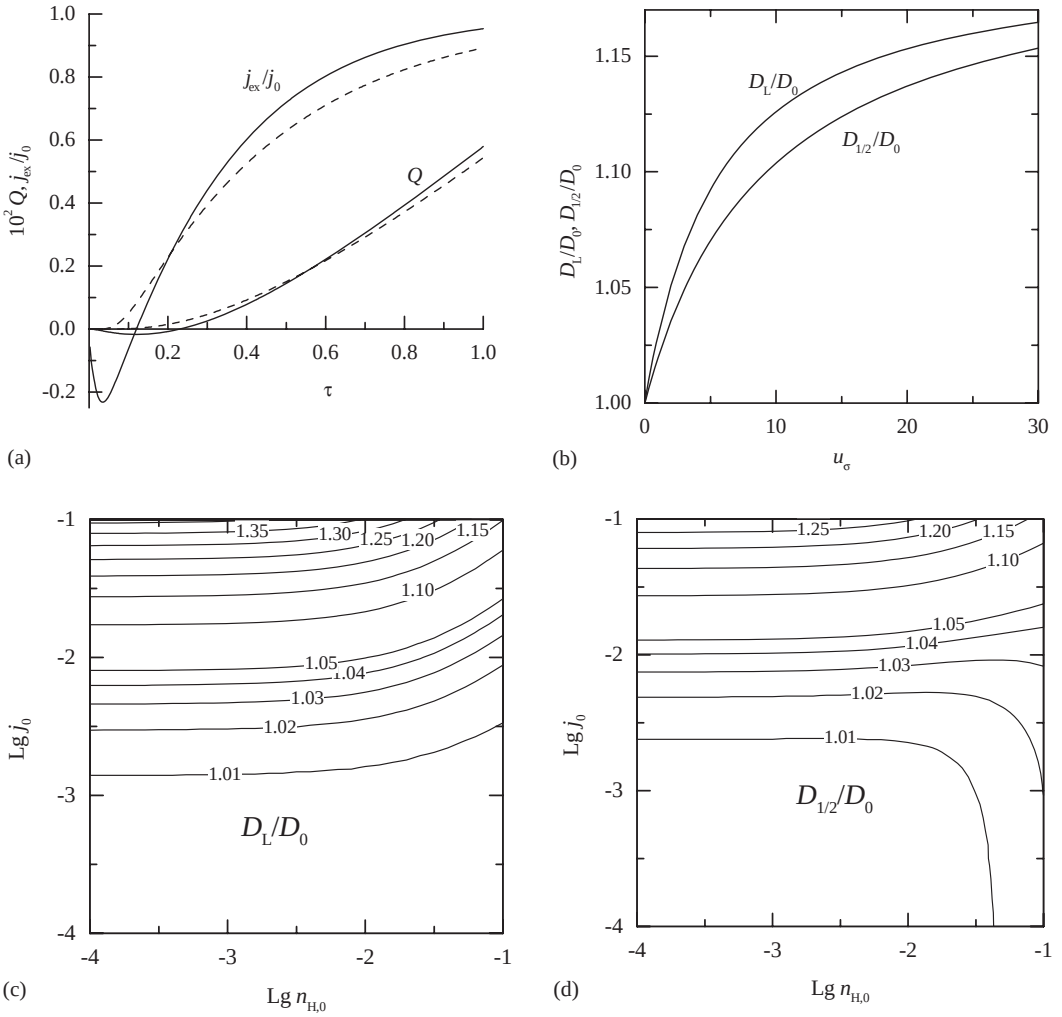

Fig. 3. Effects of various parameters on apparent diffusion coefficients under flux-step boundary conditions. (a) An example of diffusion flux and diffused quantity for the self-stress (solid curves) and stress-free situations (dashed curves); (b) the effects of self-stress factor u_σ; (c) contour map of D_L vs. $n_{H,0}$ and j_0; (d) contour map of $D_{1/2}$ vs. $n_{H,0}$ and j_0. The parameters are $n_{H,0} = 0.1$, $j_0 = 0.1$, $u_\sigma = 20$ except for independent variables in each figure.

From Figs. 2 and 3, we find that the flux-step with a small charging current gives the minimum errors in measurements of diffusion coefficient at a nonzero of $n_{H,0}$. This means that we can obtain an ADC value close to the SFDC by this method. In experiments [1,2,13–16], the hydrogen electrode reaction is along the fast Volmer-slow Tafel mechanism on Pd surface and j_0 is the same as the applied current while it is small [34]. On the other hand, the assumption of large volume V in Eqs. (11) and (20) are easily satisfied for small current. Therefore, usage of small current in the determination of diffusivity of hydrogen changing with hydrogen content is a practical method.

Although we discuss only the absorption processes, the present methods can be extended to desorption processes with boundary conditions adopted. The qualitative conclusion should be the same as here except for some quantitative modifications.

In the experiments, the behavior of j and Q may be complicated by the isometric nature of vessels besides the boundary conditions discussed in Section 3. The pressure does not change linearly with τ while it is long enough. Actually, the diffused flux will reduce to zero and the pressure in the tube will approach a steady value when the diffusion time is long enough [11]. In the experiments, if $\Delta p/p_0 \ll 1$ is not satisfied while $\tau \sim 3$, the measured ADC will differ prominently from the SFDC.

Another factor omitted is the interaction between hydrogen atoms in metals (alloys) due to the confinement of discussion on the dilute solid solution here; otherwise, this factor will induce the diffusivity changing with the hydrogen

concentration and the UHD effects will mix with the non-ideal interaction in diffusivity measurements for the metal hydride situation [33].

On the other hand, the present theory is aimed at the situation of tube configurations. For the circular plates used widely in experiments [32,36–41], we have proved that this model is appropriate as a primary approximation [10]; the detailed discussion on this configuration will be presented in the future. For other configurations, e.g. spheres, cylinders and plates, self-stresses must be treated separately according to the specific situations.

5. Conclusion

In this paper, we numerically calculate ADCs of hydrogen in thin tubular membranes determined by the time-lag and half-rise methods under chemopotential- and flux-step boundary conditions to simulate diffusivity measurements of hydrogen in experiments based on the self-stress theory for interstitial solutions in thin tubular shells established earlier [9]. It is found that ADCs differ from the SFDC when either the initial concentration or the chemopotential (or flux) step is large. Generally, ADCs are less than the SFDC under the chemopotential-step, i.e. the pressure-step for gas absorption or potentiostatic charging for electrochemical absorption. However, ADCs are greater than the SFDC under the flux-step, i.e. the galvanostatic charging. At the same time, we find that the self-stress effects are proportional to the partial molar volume of hydrogen in metals but inversely proportional to temperature. Our results indicate that ADCs approach the SFDC only if the initial concentration and concentration-step (or flux-step) are small enough or the temperature is high enough. In measurements of diffusion coefficient with nonzero hydrogen concentration ($n_H \neq 0$), the effective technique is using the galvanostatic charging with small current. Finally, our theoretical results are consistent with the available experimental data.

Acknowledgements

This work is supported by NSFC Nos. 20103009, 10176030 and 10145006 and the Specialized Prophasic Basic Research Project (No. 2002CCD01900) of the Ministry of Science and Technology of China.

References

[1] Lewis FA, Magennis JP, McKee SG, Ssebuwufu PJM. Hydrogen chemical potentials and diffusion coefficients in hydrogen diffusion membranes. Nature 1983;306:673–5.
[2] Baranowski B. Stress-induced diffusion in hydrogen permeation through $Pd_{81}Pt_{19}$ membranes. J Less-Common Metals 1989;154:329–53.
[3] Baranowski B. Flow, diffusion and rate processes. In: Saniutycz S, Salomon P, editors. Advances in thermodynamics, vol. 6, New York: Taylor & Francis; 1992. p. 168–88.
[4] Kandasamy K. Influences of self-induced stress on permeation flux and space–time variation of concentration during diffusion of hydrogen in a palladium alloy. Int J Hydrogen Energy 1995;20(6):455–65.
[5] Simon AM, Grzywna ZJ. On the Larché–Cahn theory for stress induced diffusion. Acta Metall Mater 1992;40(12): 3465–73.
[6] Simon AM. A criticism of the postulated quadratic steady-state concentration profile for strain gradient induced hydrogen diffusion in metallic membranes. Int J Hydrogen Energy 1997;22(1):27–30.
[7] Zhang W-S, Zhang X-W, Zhang Z-L. Steady concentration distribution of hydrogen in elastic membranes during hydrogen diffusion. J Alloys Compounds 2000;302:258–60.
[8] Zhang W-S, Zhang X-W, Zhang Z-L. Effect of self-induced stress on the steady concentration distribution of hydrogen in fcc membranes during hydrogen diffusion. Phys Rev B 2000;62(13):8884–90.
[9] Zhang W-S, Zhang Z-L, Zhang X-W. Effects of self-induced stress in tubular membranes during hydrogen diffusion. J Alloys Compounds 2002;336:170–5.
[10] Zhang W-S, Zhang Z-L. Effects of hydrogen self-stress in thin circular-plates with clamped edges. J Alloys Compounds 2002;346:176–80.
[11] Zhang W-S. Effects of electrochemical reaction and self-stress on hydrogen diffusion in tubular membranes during galvanostatic charging. J Alloys Compounds 2003; 356–357:314–7.
[12] Adrover A, Giona M, Capobianco L, Tripodi P, Violante V. Steady-state concentration profiles of hydrogen in tubular metallic membranes. Int J Hydrogen Energy 2003;28(11):1279–84.
[13] Tong XQ, Kandasamy K, Lewis FA. Influences of lattice strain gradients on hydrogen permeation through palladium membranes containing hydrogen contents in α, $\alpha + \beta$ and β phase concentration ranges. Scr Metall Mater 1990;24: 1923–8.
[14] Tong XQ, Bucur RV, Kandasamy K, Lewis FA. Strain gradient related uphill diffusion phenomena in $Pd_{77}Ag_{23}H_n$. Z Phys Chem (NF) 1993;181:225–32.
[15] Kandasamy K, Lewis FA, Magennis JP, McKee SG, Tong XQ. Correlations with p–$c(n)$–T relationship of strain gradient dependent hydrogen diffusion in $Pd_{81}Pt_{19}H_n$ membranes. Z Phys Chem (NF) 1991;171:213–30.
[16] Sakamoto Y, Tong XQ, Lewis FA. Effects of non-Fickian uphill components of permeation flux on estimations of hydrogen diffusion coefficients in the Pd/H system. Scr Metall Mater 1991;25:1629–34.
[17] Lewis FA, Baranowski B, Kandasamy K. Uphill diffusion effects induced by self-stresses during hydrogen diffusion through metallic membranes. J Less-Common Metals 1987;134:L27–31.
[18] Tong XQ, Lewis FA. Mechanical-strain-induced influences on hydrogen diffusion within $Pd_{77}Ag_{23}$ alloy membranes. J Less-Common Metals 1991;169:157–65.
[19] Tong XQ, McNicholl R-A, Kandasamy K, Lewis FA. Hydrogen permeation in stressed and strained membranes of palladium alloys. Int J Hydrogen Energy 1992;17(10): 777–81.

[20] Kandasamy K, Tong XQ, Lewis FA. Strain gradient influences on apparent dependences of hydrogen diffusion coefficients on hydrogen content in the $Pd_{81}Pt_{19}H_n$ system. J Phys: Condens Mater 1992;4:L439–46.

[21] Dudek D, Baranowski B. Influences of self-stresses on the diffusion of hydrogen through a $Pd_{81}Pt_{19}$ membrane. Polish J Chem 1995;69:1196–204.

[22] Dudek D, Baranowski B. Diffusion coefficients of hydrogen during absorption and desorption of hydrogen in $Pd_{81}Pt_{19}$ membrane Part I: time-lag method. Z Phys Chem (NF) 1998;206:21–9.

[23] Lewis FA, Tong XQ, Kandasamy K. Lattice strain gradients influences on steady-state rates of hydrogen permeation through membranes. Int J Hydrogen Energy 1993;18(6): 481–4.

[24] Tong XQ, Lewis FA. Indications of linearity deviations of steady-state concentration profiles in hydrogen permeation membranes. Int J Hydrogen Energy 1995;20(8):641–6.

[25] Zoltowski P. Effects of self-induced mechanical stress in hydrogen sorption by metals, by EIS. Electrochim Acta 1999;44(24):4415–29.

[26] Zoltowski P, Makowska E. Diffusion coefficient of hydrogen in α-phase palladium and palladium–platinum alloy. Phys Chem Chem Phys 2001;3(14):2935–42.

[27] Baranowski B, Majchrzak S, Flanagan TB. The volume increase of fcc metals and alloys due to interstitial hydrogen over a wide range of hydrogen contents. J Phys F 1971;1: 258–61.

[28] Fukai Y. The Metal–Hydrogen System, Basic Bulk Properties. Berlin: Springer; 1993. p. 95.

[29] Crank J. The mathematics of diffusion. Oxford: Clarendon; 1975. p. 33.

[30] Fullenwider MA. Electrochemical current balance with the hydrogen–palladium system. J Electrochem Soc 1975;122(5):648–50.

[31] Boes N, Züchner H. Electrochemical methods for studying diffusion, permeation and solubility of hydrogen in metals. J Less-Common Metals 1976;49:223–46.

[32] Pound BG. Electrochemical techniques to study hydrogen ingress in metals. In: Bockris JO'M, Conway BE, White RE, editors, Modern aspects of electrochemistry, vol. 25, New York: Plenum; 1993. p. 63–133.

[33] Zhang W-S, Zhang Z-L, Zhang X-W. Effect of self-stress on the hydrogen absorption into palladium hydride electrode of plate form under galvanostatic conditions. J Electroanal Chem 1999;474:130–7.

[34] Enyo M. Hydrogen electrode reaction on electrocatalytically active metals. In: Conway BE, Bockris JO'M, Yeager E, Khan SUM, White RE, editors. Kinetics and mechanism of electrode processes, vol. 7, New York: Plenum; 1983. p. 241–300.

[35] Schöneich H-G, Züchner H. Improvement of electrochemical methods for studying metal hydrogen systems. Ber Bunsenges Phys Chem 1983;87:566–70.

[36] Li JC-M. Physical chemistry of some microstructural phenomena. Metall Trans A 1978;9A:1353–80.

[37] Sakamoto Y, Tanaka H, Lewis FA, Tong XQ. Strain gradient-induced diffusion of hydrogen in palladium and nickel membranes. Int J Hydrogen Energy 1992;17(12): 965–70.

[38] Sakamoto Y, Tanaka H, Lewis FA, Tong XQ. Observations of "uphill" diffusion of hydrogen in palladium and nickel membranes by an electrochemical permeation method. Z Phys Chem (NF) 1993;181:219–24.

[39] Sakamoto Y, Tanaka H, Sakamoto F, Lewis FA, Tong XQ. Self strain gradient induced diffusion of hydrogen in Pd–Ag alloy membranes. Int J Hydrogen Energy 1995;20(1): 35–41.

[40] Sakamoto Y, Tanaka H, Lewis FA, Tong XQ, Kandasamy K. "Uphill" hydrogen diffusion effects of hydrogen interstitial strain gradients in palladium and palladium alloys. Int J Hydrogen Energy 1996;21(11–12):1025–32.

[41] Tanaka H, Sakamoto Y, Lewis FA, Tong XQ. Uphill diffusion effects during hydrogen permeation in Palladium–Cerium alloy membrane. Defect Diffus Forum 1997;141–142: 85–92.